Supporting Information

Plasmonic $W_{18}O_{49}$-photosensitized TiO_2 nanosheets with wide-range solar light harvesting

Experimental Section

Synthesis of TiO_2 Nanosheets: 2 mL of tetrabutyl titanateand and 0.8 ml of hydrofluoric acid (30% m/m) was dissolved in a mixture of 80 mL isopropanol (IPA), and the obtained mixed solution was magnetically stirred for 3 h, and then transferred to a Teflon–lined stainless steel autoclave and heated at 200 °C for 20 h. The autoclave was cool down naturally and a white precipitate was collected, washed, and dried in air.

Synthesis of $W_{18}O_{49}$ Nanocrystals: 1 mL of anhydrous WCl_6 was dissolved in a mixture of 80 mL isopropanol (IPA), and the obtained mixed solution was magnetically stirred for 1 h, and then transferred to a teflon–lined stainless steel autoclave and heated at 200 °C for 20 h. The autoclave was cool down naturally and a navy-blue precipitate was collected, washed, and dried in vacuum oven at 50 °C.

Synthesis of Hybrid $TiO_2/W_{18}O_{49}$ Nanosheets: 2 g of TiO_2 nanosheets and 0.25 mL of WCl_6 was dissolved in a mixture of 80 mL isopropanol (IPA), and the obtained mixed solution was magnetically stirred for 2 h, and then transferred to a teflon–lined stainless steel autoclave and heated at 200 °C for 20 h. The autoclave was cool down naturally and a blue product was collected, washed, and dried in vacuum oven at 50 °C. A series of samples were synthesized by adding different amounts of WCl_6.

Specifically, 0.25, 0.5, and 1.0 mL of WCl_6 were used, and the samples were named as $TiO_2/W_{18}O_{49}$-0.25, $TiO_2/W_{18}O_{49}$-0.5, and $TiO_2/W_{18}O_{49}$-1, respectively.

Characterization: XRD patterns of the products were recorded on a Bruker D8 Focus diffractometer by using CuKα radiation (λ = 1.54178 Å). Scanning electron microscopy (SEM) images and EDS spectrums were obtained on a Hitachi S–4800. Transmission electron microscopy (TEM) and high–resolution TEM (HRTEM) characterizations were performed with a Tecnai GF30 operated at 300 kV. BET measurements were carried out in Micromeritics Tristar 3020. UV–Vis–NIR absorption spectra were recorded with a Shimadzu UV-3600. Raman spectra were obtained from Renishaw in VIA. Fourier transform infrared (FTIR) spectra were obtained from THERMO Iz10. Photoluminescence spectrum measurement was performed in a Fluorolog-3-TAU fluorescence spectrophotometer with a Xe lamp at -10°C, and the excitation wavelength is 310 nm.

Photoelectrochemical Properties: photoelectrochemical measurements were carried out by using a conventional three-electrode, single-compartment glass cell fitted with a synthetic-quartz window with a potentiostat. The saturated Ag/AgCl and platinum wire were used as the reference electrode and the counter electrode, respectively. In a typical process, sample of 1 mg was dispersed in 1 mL anhydrous ethanol and then evenly grinded to slurry. The slurry was spread onto ITO glass and the exposed area was kept at 0.4 cm^2. The prepared ITO/samples was dried overnight under ambient conditions and then used as the working electrode with 0.1 M Na_2SO_4 aqueous solution as the electrolyte. The samples served as the working electrode. The potential was swept linearly at a scan rate of 1 mV s^{-1}. The photocurrent measurements was performed by using an electrochemical system (CHI-660B).

Photocatalytic Property Test: The photocatalytic activities of the TiO_2 nanosheets, $W_{18}O_{49}$ nanocrystals, and $TiO_2/W_{18}O_{49}$ hybrid nanosheets were evaluated by degradation of RhB in an aqueous solution. A 300W Xe lamp (HSX-F300, NBeT) was used as the full-spectrum light source and visible light source (with a cutoff filter L450), a W infrared lamp was used as the near-infrared light source where the $\lambda < 780$ nm were filtered. The photocatalyst (50 mg) was poured into 100 mL RhB aqueous solution (20 mg/L) in a Pyrex reactor at room temperature under air. Before light was turned on, the suspension was continuously stirred for 30 min in dark to ensure the establishment of an adsorption–desorption equilibrium. The concentration of RhB during the degradation was monitored by colorimetry using a UV-vis spectrometer (Shimadzu UV-3600).

Supported Figures

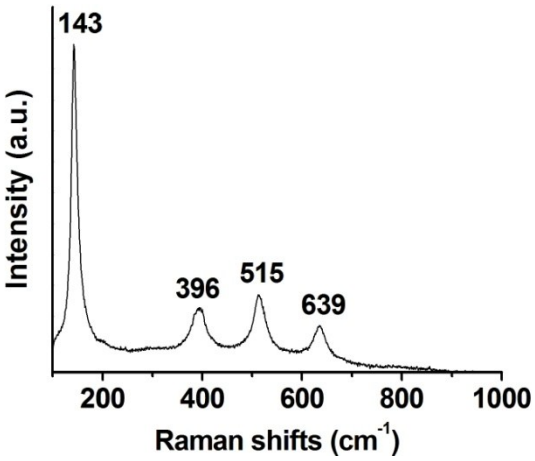

Fig. S1 Raman spectrum of the anatase phase TiO_2 nanosheet.

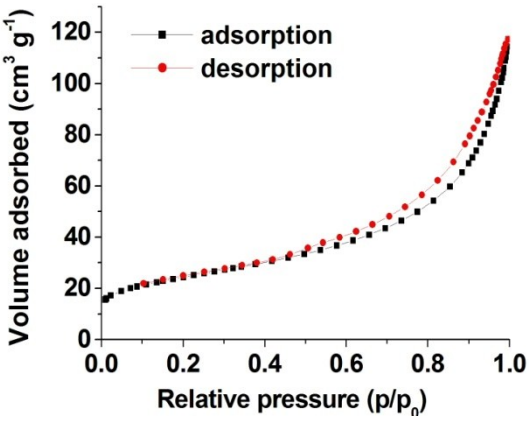

Fig. S2 N_2 adsorption/desorption isotherms of the anatase phase TiO_2 nanosheets.

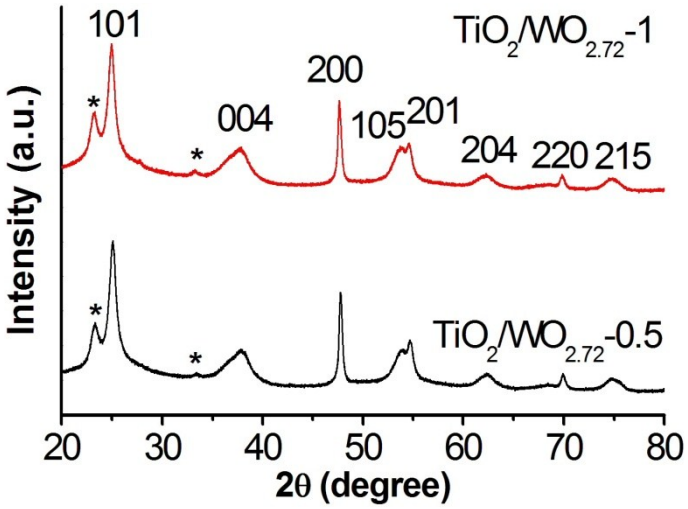

Fig. S3 XRD patterns of the samples of $TiO_2/W_{18}O_{49}$-0.5 and $TiO_2/W_{18}O_{49}$-1.

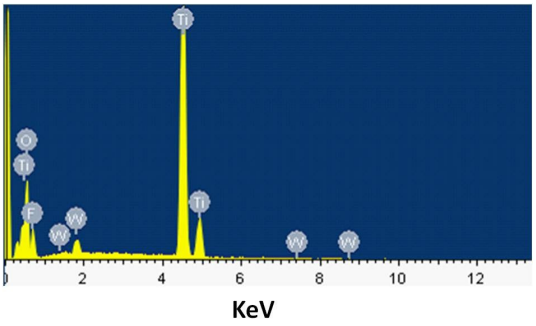

Fig. S4 EDS spectrum of the sample of $TiO_2/W_{18}O_{49}$-0.25. The F signal come from the residual F ions adsorbed in the TiO_2 nanosheets.

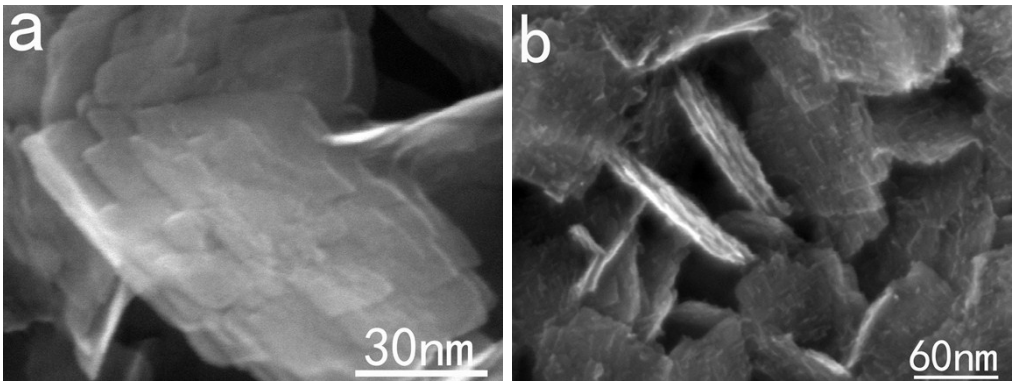

Fig. S5 SEM images of the samples of $TiO_2/W_{18}O_{49}$-0.5 (a) and $TiO_2/W_{18}O_{49}$-1.0 (b).

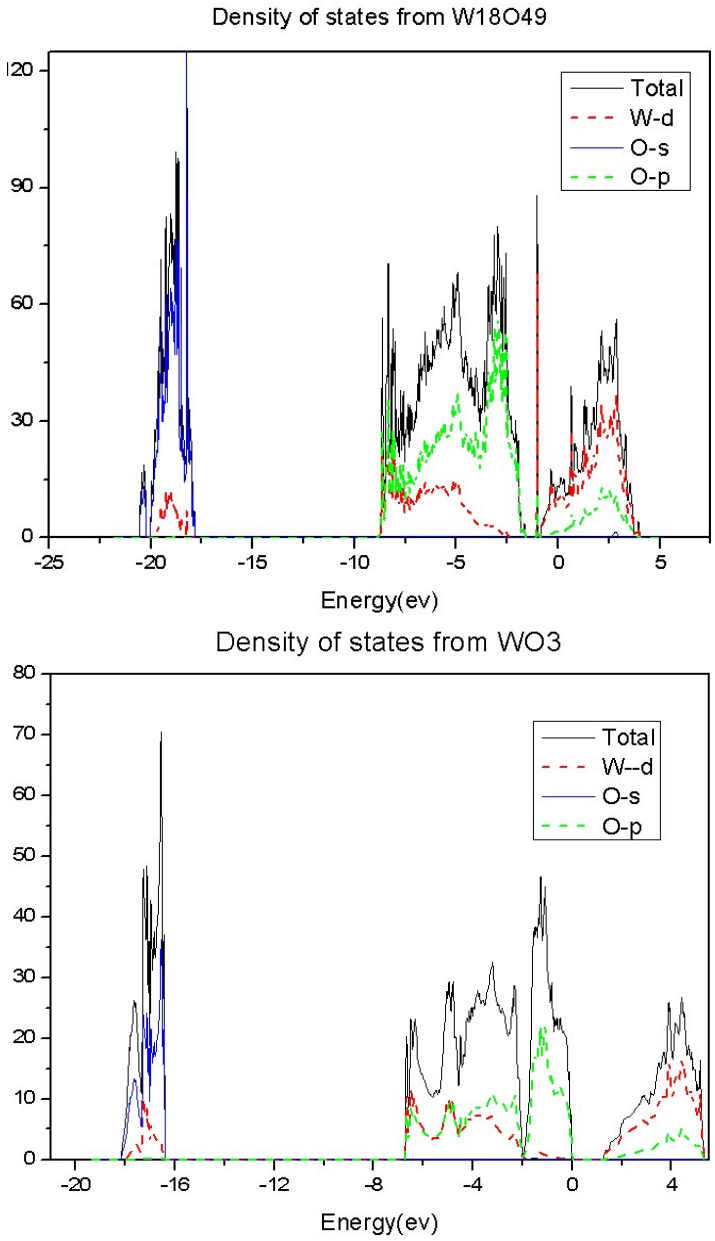

Fig. S6 Band structures of $W_{18}O_{49}$ and WO_3.

Computation Details. All the DFT calculations were carried out using the Vienna ab initio simulation package (VASP).[1-3] The energy cutoff for the plane wave basis set was 600 eV. The generalized gradient approximation (GGA) with the function of Perdew and Wang (PW91)[4] was used to deal with the exchange correlation energies. And the electron-ion interaction was described by the projected augmented wave (PAW) method.[5],For the bulk calculation, the geometry optimization was stopped when force on each atom was less than 0.01 eV/Å. Brillouin zones were sampled with Monkhorst-Pack k-points of 4 × 4 × 4, 2 × 10 × 3 for WO_3 and $W_{18}O_{49}$, respectively.

The optimized lattice constants of bulk are compiled in Table1, in reasonable agreement with the experimental and calculated values.[6-9]

The Brillouin zone sampling was carried out with the k-points of 1 × 5 × 1 for the $W_{18}O_{49}$ nanowire calculation. The atomic relaxation was stopped until the force on each atom was smaller than 0.05 eV/Å as previous report.[7A] larger 1 × 15 × 1 k-point was used for the calculations of density of states (DOS) at the DFT level. Note that pure DFT always underestimates the band gaps in comparison with the experimental values, so a hybrid functional approach implemented in the framework of Heyd-Scuseria-Ernzerh of (HSE06)[10-12] is used to obtain the electronic structures of the WO_3 and $W_{18}O_{49}$ nanowires. It is found that when using 45% (i.e, mixing parameter α=0.45)mixing of HF, a direct band gap of 2.83 eV was obtained for the WO_3 bulk, which is well consistent with the experimental gap of 2.6-3.2eV.[13-15] So this parameter is also used in the calculation of the $W_{18}O_{49}$ nanowires.

(1) Kresse, G.; Hafner, J. Physical Review B 1994, 49, 14251.

(2) Kresse, G.; Furthmüller, J. Computational Materials Science 1996, 6, 15.

(3) Kresse, G.; Furthmüller, J. Physical Review B 1996, 54, 11169.

(4) Perdew, J. P.; Chevary, J. A.; Vosko, S. H.; Jackson, K. A.; Pederson, M. R.; Singh, D. J.; Fiolhais, C. Physical Review B 1992, 46, 6671.

(5) Blöchl, P. E. Physical Review B 1994, 50, 17953.

(6) Kresse, G.; Joubert, D. Physical Review B 1999, 59, 1758.

(7) Migas, D. B.; Shaposhnikov, V. L.; Borisenko, V. E. The Journal of Apply Physics 2010, 108, 093714.

(8) Valdes, A.; Kroes, G. J. The Journal of chemical physics 2009, 130, 114701.

(9) Wang, F.; Di Valentin, C.; Pacchioni, G. The Journal of Physical Chemistry C 2012, 116, 8901.

(10) Heyd, J.; Scuseria, G. E.; Ernzerhof, M. The Journal of chemical physics 2003, 118, 8207.

(11) Heyd, J.; Scuseria, G. E. The Journal of chemical physics 2004, 121, 1187.

(12) Heyd, J.; Scuseria, G. E.; Ernzerhof, M. The Journal of chemical physics 2006, 124, 219906.

(13) Niklasson, G. A.; Granqvist, C. G. The Journal of Material Chemistry 2007, 17, 127.

(14) Zheng, H.; Ou, J. Z.; Strano, M. S.; Kaner, R. B.; Mitchell, A.; Kalantar-zadeh, K. Advance Function Materials 2011, 21, 2175.

(15) Vemuri, R. S.; Engelhard, M. H.; Ramana, C. V. ACS applied materials & interfaces 2012, 4, 1371.

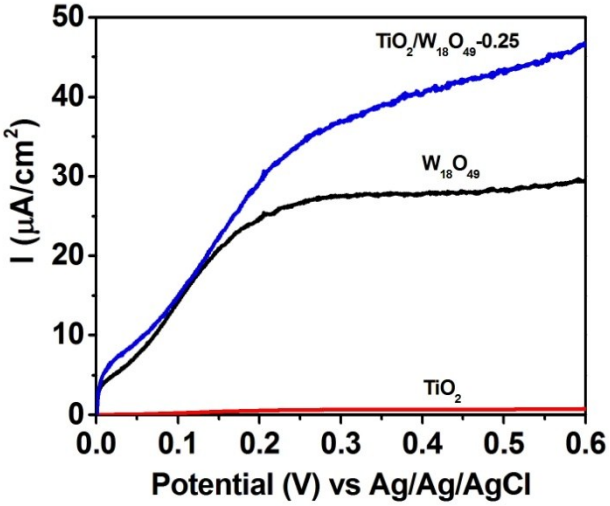

Fig. S7 Photocurrent response of the $TiO_2/W_{18}O_{49}$-0.25 hybrid nanosheets, pure TiO_2 nanosheets, and $W_{18}O_{49}$ nanocrystals under the visible-light illumination ($\lambda > 420$ nm).